A Predictability Study of a Polar Low Linked to a Tropopause Polar Vortex

Kevin Biernat[1]*, Daniel Keyser[1], Lance F. Bosart[1], and Steven M. Cavallo[2]

*E-mail: kbiernat@albany.edu

[1]*University at Albany, SUNY*

[2]*University of Oklahoma*

Presented at AGU 2018 Fall Meeting on 14 December 2018

A51I-2264

This research was supported by Office of Naval Research Grant N00014-18-1-2200

1) Background

- Tropopause polar vortices (TPVs) are tropopause-based vortices of high-latitude origin and are material features (e.g., Cavallo and Hakim 2010)
- Polar lows are small, intense cyclones characterized by short horizontal scales, lifetimes, and evolution, and often form within, or at the leading edge of, a cold air mass moving over warmer sea surfaces in high latitudes (e.g., Rasmussen and Turner 2003)
- Polar lows may be associated with strong surface winds and heavy precipitation, posing hazards to ships and infrastructure (e.g., Rasmussen and Turner 2003)
- TPVs may act as precursors for the development of polar lows (e.g., Kolstad 2011)
- This study investigates physical processes that influence the evolution and predictability of a polar low linked to a TPV

2) Data and Methods

- Obtained polar lows from the Sea Surface Temperature and Altimeter Synergy for Improved Forecasting of Polar lows (STARS) database of polar lows over the Norwegian and Barents Sea during 2002–2011 (Sætra et al. 2010)
- Compared STARS database to a 1979–2015 database of TPVs constructed using the ERA-Interim (Dee et al. 2011) and a TPV tracking algorithm (Szapiro and Cavallo 2018), and identified polar lows linked to TPVs
- Conducted a multiscale analysis of a Barents Sea polar low linked to a TPV occurring during 1800 UTC 10–1200 UTC 11 February 2011 using the ERA5 (Hersbach and Dee 2016)
- Used the ECMWF Ensemble Prediction System (Buizza et al. 2007) initialized at 1200 UTC 9 February 2011 (30 h prior to polar low genesis) to evaluate the forecast skill of the polar low, with the ERA5 used as the verification
- Assessed forecast skill of polar low in terms of a metric adapted from Lamberson et al. (2016) that combines forecast track and intensity error of polar low based on 850-hPa relative vorticity, ζ
- Separated ensemble members into two groups: the eight most accurate and the eight least accurate members in terms of the aforementioned metric

3) Climatology and Case Tracks

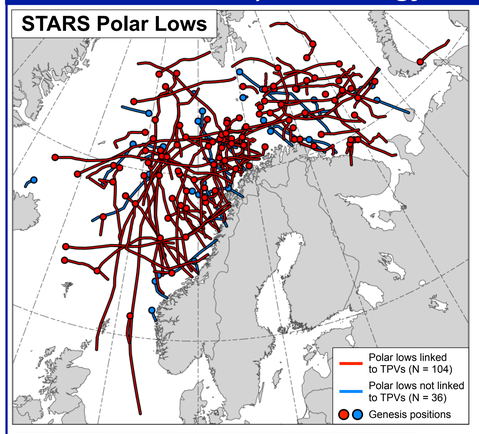

Fig. 1 (left). Tracks of STARS polar lows linked to TPVs (red) and STARS polar lows not linked to TPVs (blue). Dots indicate the genesis locations of the polar lows. 104 out of a total 140 polar lows, or 74.3%, are linked to TPVs.

Table 1. Lifetimes of polar low (PL) and TPV of interest

Feature	Date of Genesis	Date of Lysis	Lifetime
PL	10 Feb 2011	11 Feb 2011	18 h
TPV	31 Jan 2011	20 Feb 2011	20 d

Figure 2 (below). Tracks of (a) polar low and (b) TPV, and 10–11 Feb 2011 time-mean (a) 850-hPa temperature (°C, gray) and standardized temperature anomalies (σ, shaded), and (b) 300-hPa geopotential height (dam, gray) and standardized geopotential height anomalies (σ, shaded). 0000 UTC positions (every 48 h) of TPV shown by dots, and numbers represent dates corresponding to the 0000 UTC positions.

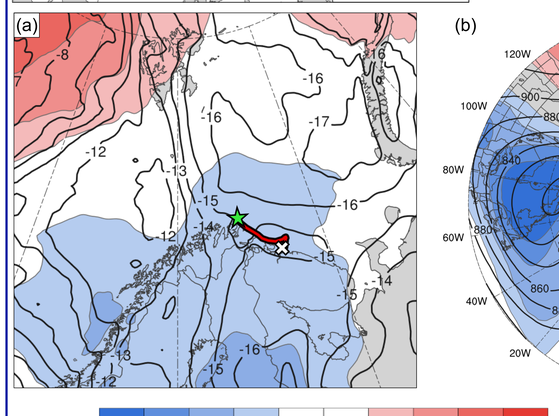

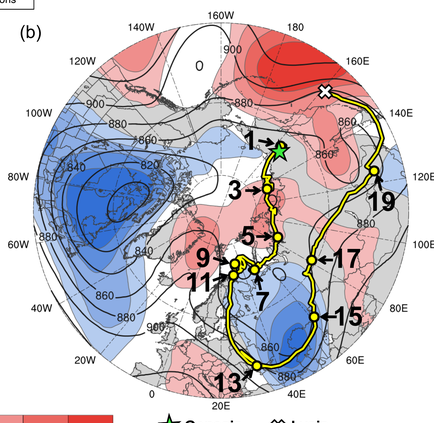

4) Polar Low and TPV Evolution

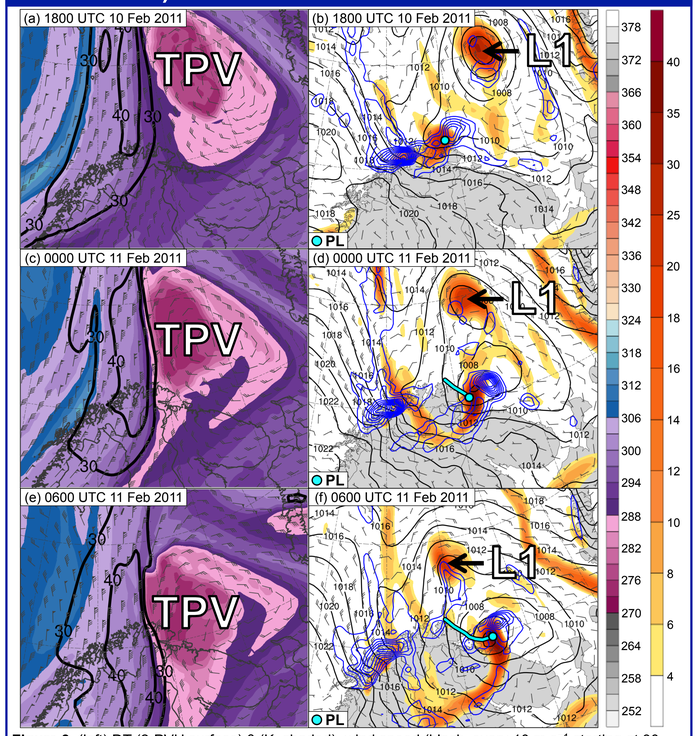

Figure 3. (left) DT (2-PVU surface) θ (K, shaded), wind speed (black, every 10 m s^{-1} starting at 30 m s^{-1}), and wind (m s^{-1}, flags and barbs); (right) 850-hPa ζ (10^{-5} s^{-1}, shaded), 850–600-hPa ascent (blue, every 2.5 × 10^{-3} hPa s^{-1}), SLP (hPa, black), and 10-m wind (m s^{-1}, barbs). "L1" and "TPV" denote positions of a predecessor cyclone (L1) and the TPV, respectively.

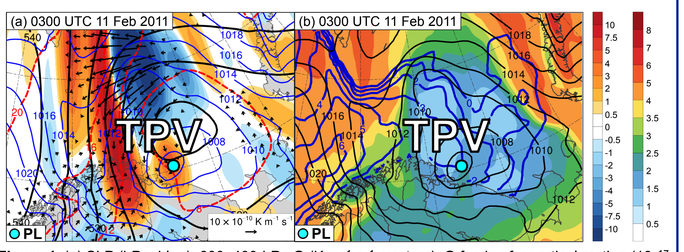

Figure 4. (a) SLP (hPa, blue); 600–400-hPa **Q** (K m^{-1} s^{-1}, vectors), **Q** forcing for vertical motion (10^{-17} Pa^{-1} s^{-3}, shaded), θ (°C, red), and geopotential height (dam, black); (b) 900–600-hPa static stability [K (100 hPa)$^{-1}$, shaded], SLP (hPa, black), and SST (°C, blue). "TPV" denotes position of TPV.

5) Ensemble Track and Intensity

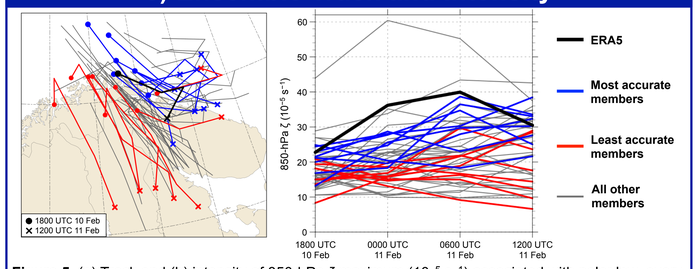

Figure 5. (a) Track and (b) intensity of 850-hPa ζ maximum (10^{-5} s^{-1}) associated with polar low, every 6 h during 1800 UTC 10–1200 UTC 11 Feb 2011.

References

- Buizza, R., J. R. Bidlot, N. Wedi, M. Fuentes, M. Hamrud, G. Holt, and F. Vitart, 2007: The new ECMWF VAREPS (Variable Resolution Ensemble Prediction System). *Quart. J. Roy. Meteor. Soc.*, **133,** 681–695.
- Cavallo, S. M., and G. J. Hakim, 2010: Composite structure of tropopause polar cyclones. *Mon. Wea. Rev.*, **138,** 3840–3857.
- Dee, D. P., and Coauthors, 2011: The ERA-Interim reanalysis: Configuration and performance of the data assimilation system. *Quart. J. Roy. Meteor. Soc.*, **137,** 553–597.
- Hersbach, H., and D. Dee, 2016: ERA5 reanalysis is in production. *ECMWF Newsletter*, No. 147, ECMWF, Reading, United Kingdom, 7. [Available online at www.ecmwf.int/sites/ default/files/elibrary/2016/16299-newsletter-no147-spring-2016.pdf.]
- Kolstad, E. W., 2011: A global climatology of favourable conditions for polar lows. *Quart. J. Roy. Meteor. Soc.*, **137,** 1749–1761.
- Lamberson, W. S., R. D. Torn, and L. F. Bosart, 2016: Diganosis of the source and evolution of medium-range forecast errors for Extratropical Cyclone Joachim. *Wea. Forecasting*, **31,** 1197–1214.
- Rasmussen, E., and J. Turner, 2003: *Polar Lows: Mesoscale Weather Systems in the Polar Regions.* Cambridge University Press, 612 pp.
- Szapiro, N., and S. Cavallo, 2018: TPVTrack v1.0: A watershed segmentation and overlap correspondence method for tracking tropopause polar vortices. *Geosci. Model Dev. Discuss.*, in review.
- Sætra, Ø., Y. Gusdal, S. Eastwood, J. Debernard, P.-E. Isachesen, H. Schyberg, B. Furevik, and G. Noer, 2010: Scientific analysis plan (d3). Tech. Rep., Norwegian Meteorological Institute, 49 pp.

6) Ensemble Differences at 1800 UTC 10 Feb 2011 (30-h Forecast)

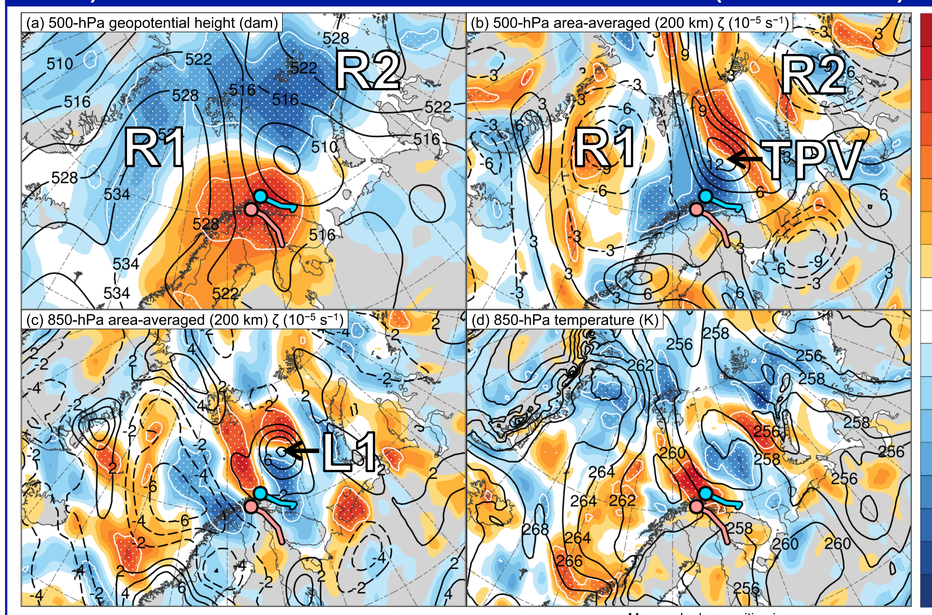

Ensemble mean

shading: normalized composite differences (σ; most accurate group minus least accurate group)

stippling: statistically significant differences between groups at 95% confidence level according to a two-sided Student's *t* test

Mean polar low position in most accurate group*

Mean polar low position in least accurate group*

***Track:** 1800 UTC 10–1200 UTC 11 Feb 2011

Figure 6. Fields as specified above at 1800 UTC 10 Feb 2011. Normalized composite differences calculated using the equation below, adapted from Lamberson et al. (2016). "R1," "R2," "L1," and "TPV" denote ensemble-mean positions of ridge 1 (R1), ridge 2 (R2), L1, and TPV, respectively.

$$\Delta x_i = \frac{\overline{\mathbf{x}}_i^{\,most\ accurate} - \overline{\mathbf{x}}_i^{\,least\ accurate}}{\sigma_{x_i}}$$

$\overline{\mathbf{x}}_i^{\,most\ accurate}$ = mean of ith state variable for most accurate members

$\overline{\mathbf{x}}_i^{\,least\ accurate}$ = mean of ith state variable for least accurate members

σ_{x_i} = ensemble standard deviation of $\mathbf{x}_i$ computed for all members

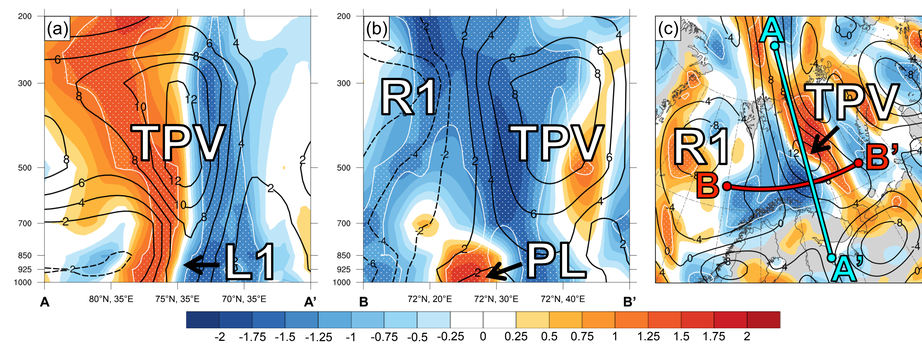

Figure 7. Cross sections along (a) AA' and (b) BB' of area-averaged (200 km) ζ, and (c) plan-view map of 500-hPa area-averaged (200 km) ζ at 1800 UTC 10 Feb 2011. Contours, shading, and stippling as in Fig. 6. "TPV", "R1", "L1", and "PL" denote ensemble-mean positions of TPV, R1, L1, and polar low, respectively. Transects for AA' and BB' shown in (c).

7) Discussion

- A large percentage, 74.3%, of the STARS polar lows are linked to TPVs (Fig. 1)
- The evolution of the polar low appears to be related to the interaction between the TPV and a tropospheric-deep baroclinic zone (Figs. 2a,b and Figs. 3a–f)
- Forcing for ascent associated with the TPV (Fig. 4a) and a favorable thermodynamic environment (Fig. 4b) likely support the intensification of the polar low (Figs. 3b,d,f)
- The polar low is stronger and positioned farther northeastward in the most accurate group compared to the least accurate group (Figs. 5a,b)
- Composite differences between the most and least accurate groups suggest that the TPV and a predecessor cyclone (L1; Figs. 3b,d,f) are positioned farther northeastward (Figs. 6a–c and Figs. 7a,b) and the tropospheric-deep baroclinic zone is positioned farther eastward (Fig. 6d) in the most accurate group
  - These position differences may be tied to the ridges flanking the TPV (R1 and R2) being less amplified (Fig. 6a) and R1 extending farther eastward (Figs. 6a,b and Fig. 7b) in the most accurate group
  - These position differences likely contribute to the polar low position differences between the groups
- A more conducive thermodynamic environment in most accurate group, as suggested by a polar low track mainly over the Barents Sea (Figs. 6a–d), may contribute to polar low being stronger in most accurate group